Dimer-hole-RVB state of the two-leg t-J ladder: A recurrent variational ansatz

Germán Sierra*
Institute for Theoretical Physics, University of California, Santa Barbara, California 93106

Miguel Angel Martín-Delgado†
Departamento de Física Teórica I, Universidad Complutense, 28040 Madrid, Spain

Jorge Dukelsky‡
Instituto de Estructura de la Materia, C.S.I.C., 28006 Madrid, Spain

Steven R. White§
Department of Physics and Astronomy, University of California, Irvine, California 92697

D. J. Scalapino‖
Department of Physics, University of California, Santa Barbara, California 93106

(Received 31 July 1997; revised manuscript received 14 October 1997)

We present a variational treatment of the ground state of the two-leg t-J ladder, which combines the dimer and the hard-core boson models into one effective model. This model allows us to study the local structure of the hole pairs as a function of doping. A second-order recursion relation is used to generate the variational wave function, which substantially simplifies the computations. We obtain good agreement with numerical density matrix renormalization group results for the ground state energy in the strong-coupling regime. We find that the local structure of the pairs depends upon whether the ladder is slightly or strongly dopped. [S0163-1829(98)06817-9]

INTRODUCTION

The two-leg, t-J ladder represents one of the simplest systems which exhibits some of the phenomena associated with high-T_c cuprate superconductivity.[1–6] The ground state of the undoped system, a two-leg Heisenberg ladder, is a spin liquid with a finite spin gap and exponentially decaying antiferromagnetic spin-spin correlations. Upon doping, the spin gap remains and there appear power law charge density wave (CDW) and singlet superconducting (SC) pairing correlations. In addition, the pairing correlations have an internal $d_{x^2-y^2}$-like symmetry with a relative sign difference between the leg and rung singlets which make up a pair. Despite all of the numerical and analytical work which has been done on this system, we still lack a picture of the ground state which accommodates all of these physical properties. There are, however, many hints of what that picture may look like. It is the purpose of this paper to take one step further in that direction.

Short-range resonating valence bonds (RVB's) provide a useful basis for representing the ground state of spin liquids.[7,8] For the t-J ladder, a zeroth-order picture has been provided by the study of the strong-coupling limit where the exchange coupling constant along the rungs, J', is much larger than any other scale in the problem. The other coupling constants of the model are J, the exchange coupling constant along the legs, and t and t', the hopping parameters along the legs and the rungs, respectively. In the limit $J' \gg J,t,t'$, the ground state of the undoped ladder is simply given by the coherent superposition of singlets across the rungs. The addition of one hole requires the breaking of one of these singlets, in which case the hole gets effectively bound to the unpaired spin, becoming a quasiparticle with spin 1/2 and charge $|e|$. The addition of another hole leads to the binding of two holes in the same rung in order to minimize the cost in energy. In this picture there is no spin-charge separation, a fact that remains valid down to intermediate and weak couplings, as confirmed by various numerical and analytical studies. Based on this picture it is possible to construct an effective theory describing the motion and interactions of the hole pairs.[6] It is given by a hard-core boson (HCB) model characterized by an effective hopping parameter t^* and interaction V^* of the hole pairs. The HCB model describes the doped ladder as a Luther-Emery liquid, with gapped spin excitations and gapless charge collective modes, which are responsible for the CDW and SC power law correlations. We summarize the zeroth-order picture in Fig. 1, which shows a typical state of HCB's, as well as the two building blocks that are used its construction.

In order to go beyond this picture, we need to consider the fluctuations of the states of the HCB model. To lowest order in perturbation theory they are shown in Fig. 2. The admixture of the state shown in Fig. 2(a) is of order J/J' and represents a resonance of two nearest-neighbor rung singlets.

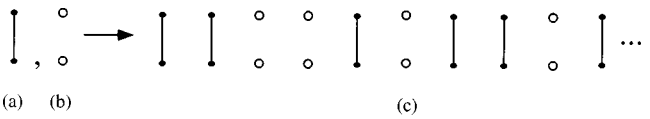

FIG. 1. The zeroth-order picture of the hard-core boson model: (a) the vertical bond, (b) the vertical hole-pair singlet, and (c) a typical state of the HCB model.

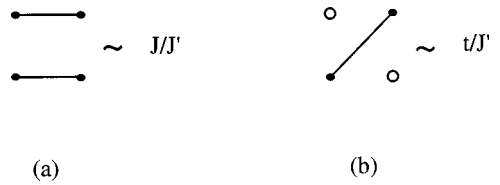

FIG. 2. The two lowest-order states in the strong-coupling limit $J' \gg J,t,t'$ of the HCB model; they represent the first-order contribution to the DHCB model: (a) the resonance of two vertical bonds and (b) bound state of two quasiparticles.

According to the standard RVB scenario, this resonance effect leads to a substantial lowering of the ground state energy. The state in Fig. 2(b) is of order t/J', and it can be thought of as a bound state of two quasiparticles, whose characteristic feature is the diagonal frustrating bond across the holes. From the RVB point of view, Fig. 2(b) is a resonance of a singlet and a hole pair. The importance of this state, even for intermediate couplings such as $J=J'=0.5t$, was emphasized in the density matrix renormalization group (DMRG) study of Ref. 9, where it was shown to be the most probable configuration of two dynamical holes in a two-leg ladder. In the HCB model of Ref. 6, the states of the form of Fig. 2(b) are taken into account as intermediate or virtual states, which lead to the effective hopping t^* and interaction V^* between the hole pairs. It is clear, however, that ''integrating out'' the diagonal states through perturbation theory erases the internal structure of the hole pairs. Here we want to extend the HCB description to include the internal structure of the hole pairs.

In order to define an effective model which would retain the degrees of freedom associated with the internal structure of the hole pairs, we need to consider the states that appear in second order in the strong-coupling expansion. They are given in Fig. 3. Let us comment on them. The state of Fig. 3(a) is of order $(J/J')^2$ and it is a higher-order RVB state, whose contribution to the ground state of the undoped ladder was studied in Ref. 10. In this reference it was shown that its inclusion in a variational ansatz improves the numerical results, but does not change the qualitative picture obtained using the dimer ansatz.[4,11] The state of Fig. 3(b), which is in fact first order in t', can be seen as a bound state of two

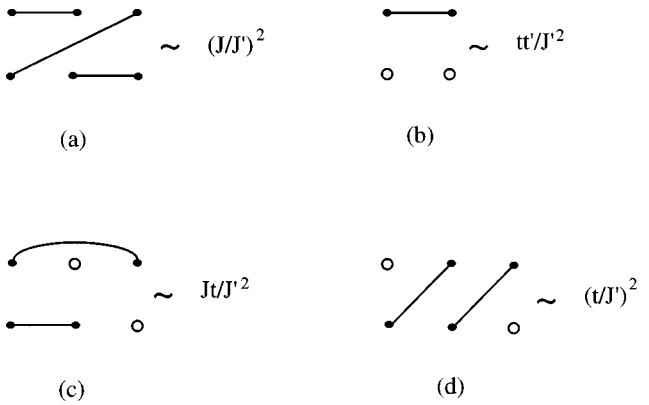

FIG. 3. Higher-order strong-coupling states contributing to the DHCB model: (a) a higher-order RVB state, (b) a bound state of two quasiparticles, and (c) and (d) higher-order corrections to the diagonal state (b).

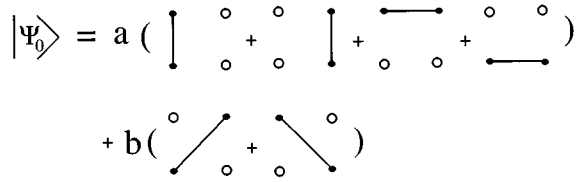

FIG. 4. The exact ground state for a single plaquette with two holes (Ref. 9) (case $N=2$ and $P=1$).

quasiparticles, while Figs. 3(c) and 3(d) are higher-order corrections to the diagonal state shown in Fig. 2(b). For these reasons it seems consistent to keep the state of Fig. 3(b) on an equal footing with the states of Figs. 2(a) and 2(b). To give further support to this choice, we notice that the exact solution for two holes on the 2×2 cluster requires a superposition of the states shown in Figs. 2(b) and 3(b) along with Figs. 1(a) and 1(b) (see Fig. 4).[9]

In summary, we conjecture that in order to discuss the nature of the superconducting order parameter of the doped two-leg, t-J ladder, in the strong-coupling regime, it is sufficient to consider states built up from five possible local configurations, given by rung-singlet bonds [Fig. 1(a)], rung-hole pairs [Fig. 1(b)], two-leg bonds [Fig. 2(a)], hole pairs with a singlet diagonal bond [Fig. 2(b)] and hole pairs with a singlet leg bond [Fig. 3(b)]. A typical state constructed using these building blocks is shown in Fig. 5. We shall call these types of states *dimer-hole-RVB* states. The effective model that governs their dynamics will be called the *dimer hard-core boson model* (DHCB) and its Hamiltonian can be determined by considering the fluctuations of the dimer-hole states, in a manner similar to the one considered above for the HCB states. The DHCB model contains spin and charge degrees of freedom, together with their couplings, and in that sense is an interesting model to study the interplay between the two types of degrees of freedom, although here we will focus on the variational ground state of the model.

The mathematical formulation of the DHCB model involves an interesting but complicated combination of vertex and interaction round a face (IRF) models. The latter terminology is borrowed from statistical mechanics.[12] The vertex variables describe the number of electrons per rung, i.e., $n_i=0,1,2$, while the IRF variables describe the number and type of bonds connecting two rungs, i.e., $l_{i,i+1}=0$, 1_d, 1_h, 2, where the subindices d and h indicate the diagonal or horizontal nature of the bond. The only allowed configurations for two consecutive IRF variables $(l_{i,i+1},l_{i+1,i+2})$ are $(0,0)$, $(1_d,0)$, $(1_h,0)$, and $(2,0)$ together with their permutations. Moreover, the vertex variables are subject to certain constraints imposed by the IRF ones. Namely, (A) if $l_{i,i+1}=1_d$ or 1_h, then $n_i=n_{i+1}=1$, and (B) if $l_{i,i+1}=2$, then $n_i=n_{i+1}=2$. Only if $l_{i,i+1}=0$ can n_i and n_{i+1} take any value, i.e., 0, 1, or 2.

It is beyond the scope of this work to present a full account of the DHCB model. Instead, we shall try to uncover

FIG. 5. A typical dimer-hole-RVB state.

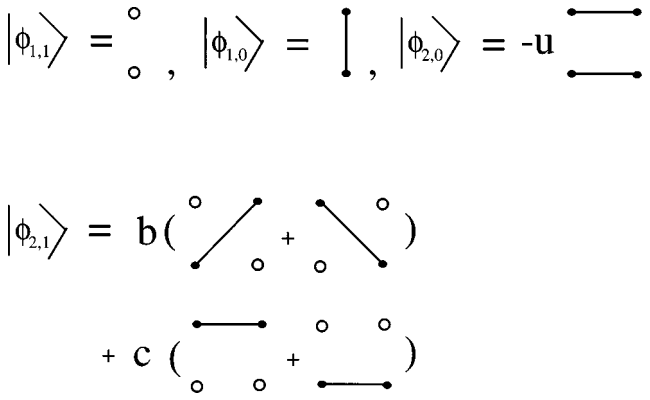

FIG. 6. Elementary building block states of the RRM used in the construction of the dimer-hole states.

some of its physics, by means of a combination of two approaches, namely, the density matrix renormalization group method[13] and the recurrence relation method (RRM).[10] While the DMRG method is a powerful numerical technique, which in many cases yields the exact answer, the RRM is essentially analytic, lacking the numerical precision of the DMRG method, but sharing with it some features, such as, for example, the Wilsonian way of growing the system by the addition of sites at the boundary. In the RRM one begins with an assumption about the local configurations through which the system grows. Then one may test whether the state that is generated gives results in agreement with the essentially exact DMRG results.

VARIATIONAL WAVE FUNCTION

The Hamiltonian of the two-leg, t-J ladder is given by

$$\mathcal{H}=\mathcal{H}_S+\mathcal{H}_K=\sum_{\langle i,j\rangle} J_{ij}(\mathbf{S}_i\cdot\mathbf{S}_j-\tfrac{1}{4}n_in_j)$$

$$-\sum_{\langle i,j\rangle,s} t_{ij}P_G(c^\dagger_{i,s}c_{j,s}+c^\dagger_{j,s}c_{i,s})P_G, \qquad (1)$$

where $J_{ij},t_{ij}=J,t$ or J',t', depending on whether the link $\langle ij\rangle$ is along the legs or the rungs, respectively. P_G is the Gutzwiller projection operator which forbids double occupancy. The rest of the operators appearing in Eq. (1) are standard (we use the conventions of Ref. 9). Each site i is labeled by the coordinates (x,y) with $x=1,\ldots,N$ and $y=1,2$. We choose open boundary conditions along the legs of the ladder.

The pair field operator which creates a pair of electrons, at the sites i and j, out of the vacuum is given by

$$\Delta^\dagger_{i,j}=\frac{1}{\sqrt{2}}(c^\dagger_{i,\uparrow}c^\dagger_{j,\downarrow}+c^\dagger_{j,\uparrow}c^\dagger_{i,\downarrow}). \qquad (2)$$

As explained in the Introduction, we want to build up an ansatz for the ground state based on the five local configurations of the DHCB model. The explicit realization of these configurations in terms of pair field operators are given by (see Fig. 6),

$$|\phi_{1,1}\rangle_x=|0\rangle_x,$$

$$|\phi_{1,0}\rangle_x=\Delta^\dagger_{(x,1)(x,2)}|0\rangle_x,$$

$$|\phi_{2,0}\rangle_{x,x+1}=-u\Delta^\dagger_{(x,1)(x+1,1)}\Delta^\dagger_{(x,2)(x+1,2)}|0\rangle_{x,x+1}, \qquad (3)$$

$$|\phi_{2,1}\rangle_{x,x+1}=[b(\Delta^\dagger_{(x,1)(x+1,2)}+\Delta^\dagger_{(x,2)(x+1,1)})$$

$$+c(\Delta^\dagger_{(x,1)(x+1,1)}$$

$$+\Delta^\dagger_{(x,2)(x+1,2)})]|0\rangle_{x,x+1},$$

where $|0\rangle_x$ is the Fock vacuum associated with the rung labeled by the coordinate x ($|0\rangle_{x,x+1}=|0\rangle_x\otimes|0\rangle_{x+1}$). The states $|\phi_{n,p}\rangle$ involve $n=1,2$ rungs and $p=0,1$ pairs of holes. The variational parameter u gives the amplitude of the resonance of a pair of bonds between vertical and horizontal positions,[10] while b and c are the variational parameters associated with the diagonal and horizontal configurations of two holes, respectively. In the strong-coupling limit $J'\gg J,t,t'$, we expect to find $u\sim J/J'$, $b\sim t/J'$, and $c\sim tt'/J'^2$.

Let us call $|N,P\rangle$ the ground state of a ladder with N rungs and P pairs of holes. Of course we should be in a regime of the coupling constants where there is binding of two holes. The state $|N,P\rangle$ will be in general a linear superposition of the dimer-hole states of Fig. 5, which suggests that working with this sort of states could be a formidable task. Fortunately, we can apply the method developed in Ref. 10 to generate $|N,P\rangle$ in a recursive manner, in terms of the states of the ladders with $N-1$ and $N-2$ rungs, and P and $P-1$ pairs of holes. In Ref. 10 it was shown that $|N,P=0\rangle$, which is in fact a dimer-RVB state,[4,11] can be generated by a second-order recursion relation. Then by a simple procedure one can compute overlaps and expectation values of different operators using recursion formulas, whose thermodynamic limit can be studied analytically.

Following the strategy of considering first the HCB states and then the DHCB ones, we shall give the rule that generates the former type of states. It is given by the first-order recursion relation

$$|N+1,P+1\rangle=|N,P+1\rangle|\phi_{1,0}\rangle_{N+1}+|N,P\rangle|\phi_{1,1}\rangle_{N+1}, \qquad (4)$$

supplemented with the initial conditions

$$|1,0\rangle=|\phi_{1,0}\rangle,$$

$$|1,1\rangle=|\phi_{1,1}\rangle,$$

$$|N,P\rangle=0 \text{ for } N<P. \qquad (5)$$

Calling $F^{\mathrm{HCB}}_{N,P}$ the number of linearly independent states contained in $|N,P\rangle$, we deduce from Eq. (4) the recursion relation

$$F^{\mathrm{HCB}}_{N+1,P+1}=F^{\mathrm{HCB}}_{N,P+1}+F^{\mathrm{HCB}}_{N,P}, \qquad (6)$$

whose solution is given by the combinatorial number

$$F^{\mathrm{HCB}}_{N,P}=\binom{N}{P}. \qquad (7)$$

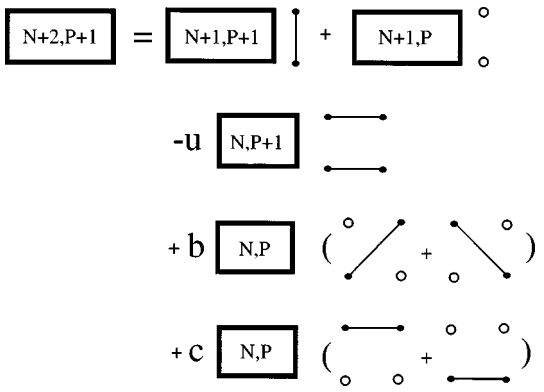

FIG. 7. A pictorial representation of Eq. (8).

Equation (7) is the dimension of the Hilbert space of the HCB model with N sites and P pair of holes. We have not introduced variational parameters in Eqs. (5), but if we did, then all states of the Hilbert space of the HCB model would be generated by the first-order recursion relation. It may be worthwhile to recall that the HCB model is essentially equivalent to the spinless fermion model or the XXZ model, which is exactly solvable by Bethe ansatz methods.[6]

Turning now to the DHCB model, the key point is to realize that the dimer-hole states can be generated by the following second-order recursion relation, involving the local configurations given by Eq. (3):

$$\begin{aligned}|N+2,P+1\rangle = &|N+1,P+1\rangle|\phi_{1,0}\rangle_{N+2}+|N+1,P\rangle|\phi_{1,1}\rangle_{N+2}\\ &+|N,P+1\rangle|\phi_{2,0}\rangle_{N+1,N+2}\\ &+|N,P\rangle|\phi_{2,1}\rangle_{N+1,N+2},\end{aligned} \tag{8}$$

with the initial conditions (5). See Fig. 7 for a graphical representation of Eq. (8).

Counting dimer-hole states

Let $F_{N,P}$ denote the number of dimer-hole states of a two-leg ladder with N rungs containing P pairs of holes. According to Eq. (8) they satisfy the recursion relation

$$F_{N+2,P+1}=F_{N+1,P+1}+F_{N,P+1}+F_{N+1,P}+4F_{N,P}, \tag{9}$$

with the initial conditions

$$F_{N,N}=1,\ F_{N,P}=0 \quad \text{for } N<P. \tag{10}$$

From Eqs. (9) and (10) we deduce that $F_{N,0}$ satisfies the well-known Fibonacci recursion formula,[10] and that in the limit of very large N it grows exponentially,

$$F_{N,0}\sim\Phi_0^N \quad (N\gg 1), \tag{11}$$

where $\Phi_0=\frac{1}{2}(1+\sqrt{5})$ is the golden ratio. Using generating function methods[10] one can easily solve the recursion relation (9), together with the initial condition (10). The result is given by the contour integral

$$F_{N,P}=\oint\frac{dz}{2\pi i}\frac{z^{N+1}(z+4)^P}{(z^2-z-1)^{P+1}}, \tag{12}$$

where the contour encircles the singularities of the integrand. For $P=0$ the integrand has two simple poles at the zeros of the polynomial z^2-z-1, the largest of which is precisely the golden ratio Φ_0. In this way one gets Eq. (11). For a finite number of holes the residue formula applied to Eq. (12) yields, to leading order in N,

$$F_{N,P}\sim N^P\Phi_0^N, \quad N\gg 1, \quad P:\text{finite}, \tag{13}$$

where the proportionality constant depends only on P. Let us finally consider the limit where both N and P go to infinity, while keeping their ratio fixed,

$$x=\frac{\text{number of holes}}{\text{number of sites}}=\frac{P}{N}, \quad 0\leq x\leq 1. \tag{14}$$

Here x can be identified with the hole doping factor of the state $|N,P\rangle$. The saddle point method applied to Eq. (12) gives the asymptotic behavior of the number of dimer-hole states for a finite density of holes,

$$F_{N,P}\sim f(x)^N, \quad f(x)=\frac{\Phi(\Phi+4)^x}{(\Phi^2-\Phi-1)^x}, \tag{15}$$

where $\Phi=\Phi(x)$ is the highest root of the following equation:

$$x=\frac{(\Phi^2-\Phi-1)(\Phi+4)}{\Phi(\Phi^2+8\Phi-3)}. \tag{16}$$

The function $f(x)$ is depicted in Fig. 8. Observe that $\Phi(0)=\Phi_0$. The effect of a finite density of holes is that of moving a singularity. This phenomenon also occurs in the computation of the energy and other observables.

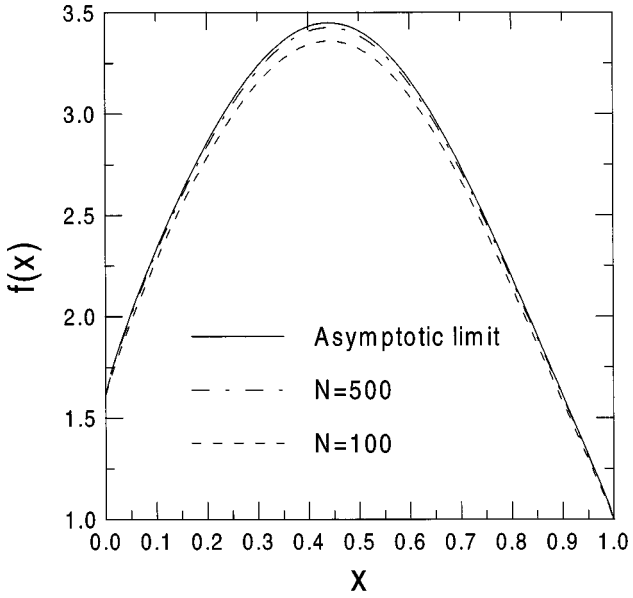

FIG. 8. The function $f(x)$ appearing in Eq. (15). The maximum appears at $x=0.44$.

Ground state energy

The parameters u,b,c are found by the standard minimization of the mean value of the energy, $\langle N,P|H_N|N,P\rangle/\langle N,P|N,P\rangle$, where H_N denotes the Hamiltonian of the ladder with N rungs. The usefulness of Eq. (8)

is that it implies that the wave function and energy overlaps also satisfy recursion relations. Let us define the following quantities:

$$
\begin{aligned}
Z_{N,P} &= \langle N,P|N,P\rangle, \\
Y_{N,P} &= {}_N\langle \phi_{1,0}|\langle N-1,P|N,P\rangle, \\
E_{N,P} &= \langle N,P|H_N|N,P\rangle, \\
D_{N,P} &= {}_N\langle \phi_{1,0}|\langle N-1,P|H_N|N,P\rangle, \\
W_{N,P} &= \langle N,P|n_N|N,P\rangle,
\end{aligned}
\tag{17}
$$

where n_N is the number operator acting on the rung N. The off-diagonal overlaps arise from the cross terms when applying Eq. (8) to the ket and the bras in $\langle N+2,P+1|N+2,P+1\rangle$ and $\langle N+2,P+1|H_{N+2}|N+2,P+1\rangle$. The recursion relations satisfied by Eq. (17) are given by

$$
\begin{aligned}
Z_{N+2,P+1} &= Z_{N+1,P+1} + u^2 Z_{N,P+1} + uY_{N+1,P+1} + Z_{N+1,P} \\
&\quad + 2(b^2+c^2)Z_{N,P}, \\
Y_{N+2,P+1} &= Z_{N+1,P+1} + u/2 Y_{N+1,P+1}, \\
E_{N+2,P+1} &= E_{N+1,P+1} - J' Z_{N+1,P+1} + u^2 E_{N,P+1} \\
&\quad - (2J+J'/2)u^2 Z_{N,P+1} + E_{N+1,P} \\
&\quad + 2(b^2+c^2)E_{N,P} - (2Jc^2 + 4bt + 8bct')Z_{N,P} \\
&\quad + uD_{N+1,P+1} - 2u(J+J'/2)Y_{N+1,P+1} \\
&\quad - 4tbY_{N+1,P} - \tfrac{1}{4} JW_{N+1,P+1} \\
&\quad - \tfrac{1}{4} Ju^2 W_{N,P+1} - \tfrac{1}{4} J(b^2+c^2)W_{N,P}, \\
D_{N+2,P+1} &= E_{N+1,P+1} - J' Z_{N+1,P+1} + u/2 D_{N+1,P+1} \\
&\quad - u(J+J'/2)Y_{N+1,P+1} - 2tbZ_{N,P} \\
&\quad - \tfrac{1}{4} JW_{N+1,P+1}, \\
W_{N+2,P+1} &= 2Z_{N+1,P+1} + 2u^2 Z_{N,P+1} + 2(b^2+c^2)Z_{N,P} \\
&\quad + 2uY_{N+1,P+1}.
\end{aligned}
\tag{18}
$$

The initial conditions read

$$
\begin{aligned}
&Z_{0,0} = 1, \quad Y_{0,0} = E_{0,0} = D_{0,0} = W_{0,0} = 0, \\
&X_{N,P} = 0, \text{ for } N < P \text{ and } X = Z,Y,E,D,W.
\end{aligned}
\tag{19}
$$

For finite values of N and P, and given choices of u,b,c, one can iterate numerically the recursion relations (18) using the initial conditions (19) and look for the minimum of the ground state energy $E_{N,P}/Z_{N,P}$. We give below the results obtained using this variational method for a 2×32 ladder and compare them with the corresponding results obtained with the DMRG method.

We also present numerical results which correspond to a variational approach to the HCB model. There are two ways to perform a variational study of the HCB model. The first one can be done in terms of the state generated by Eq. (4) and the effective HCB Hamiltonian of Ref. 6. This Hamiltonian contains the effects of virtual states of holes in diagonal positions. The other approach consists in taking $u=c=0$ and $b\neq 0$ and the full ladder Hamiltonian. We believe that both approaches give essentially the same results. We shall follow below the second one.

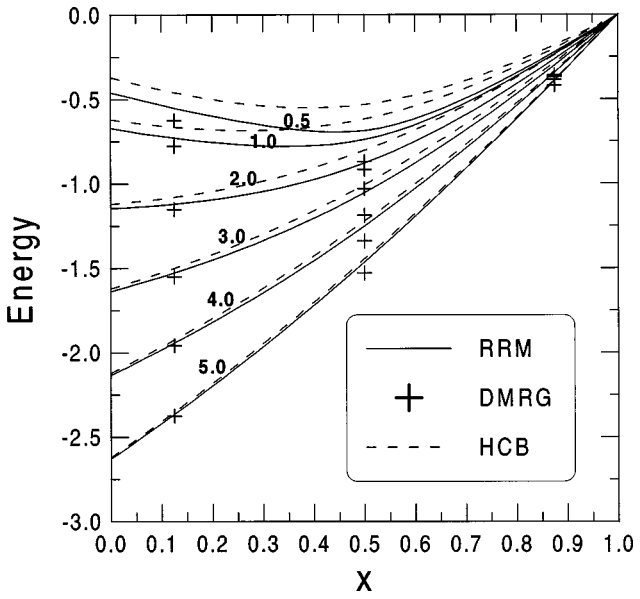

FIG. 9. Ground state energy per site of the 2×32 ladder with $J=0.5$, $t=t'=1$, and $J'=0.5,1,2,3,4,5$. The remaining data given below in Figs. 10–13 also correspond to these choices of couplings. The continuum curves are obtained with the RRM. The dotted curves correspond to the variational computation with $u=c=0$ and $b\neq 0$, which we argue gives a variational estimate of the HCB ground state energy. The special symbols are the DMRG data corresponding to $x=1/8$, 1/2, and 7/8, respectively.

RRM WAVE FUNCTION VERSUS THE DMRG METHOD: NUMERICAL RESULTS

As explained in the Introduction the DHCB model is the appropriate framework to study the strong-coupling limit of the two-leg ladder, if one wishes to take into account the local structure of the hole pairs. To check the validity of this assumption we have studied the cases where the coupling constants take the following values: $t=t'=1$, $J=0.5$, and $J'=0.5$, 1, 2, 3, 4, and 5. In this manner we go from the intermediate-coupling regime, i.e., $J'\sim 1$, to the strong-coupling regime $J'\gtrsim 3.5$. We are always working in a non-phase-separated region.

In Fig. 9 we show the ground state energy of the 2×32 ladder, for the previous choices of parameters, computed with the RRM for all dopings and the DMRG method for $x=1/8$, 1/2, and 7/8. One sees that the results obtained with the DHCB method wave function agree reasonably well with those of the DMRG and their accuracy improves as J' increases. The curve denoted as HCB corresponds to a minimization with $u=c=0$ and $b\neq 0$, and describes essentially the results of the variationally HCB state, as was explained above. We observe that the DHCB and the HCB agree very well in the strong-coupling regime $J'>>J$ and low and high dopings.

The kinetic energy of the ladder is shown in Fig. 10. It has

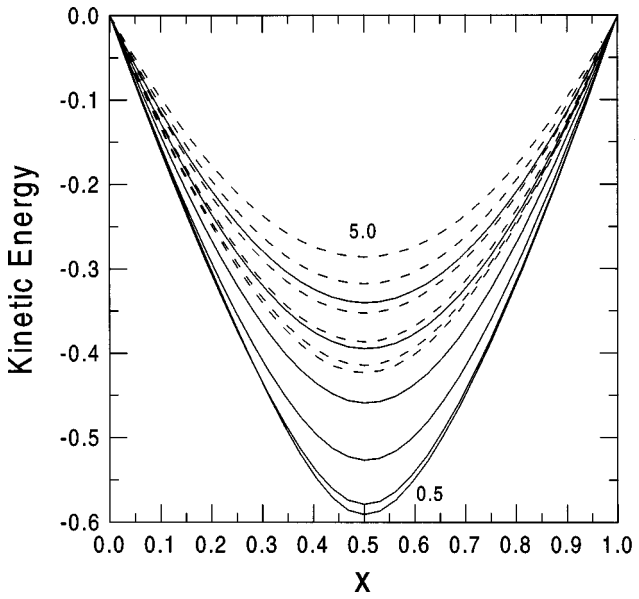

FIG. 10. Kinetic energy per site. The continuum curves correspond to the RRM, and the dotted curves correspond to the variational case $u=c=0$, $b\neq 0$.

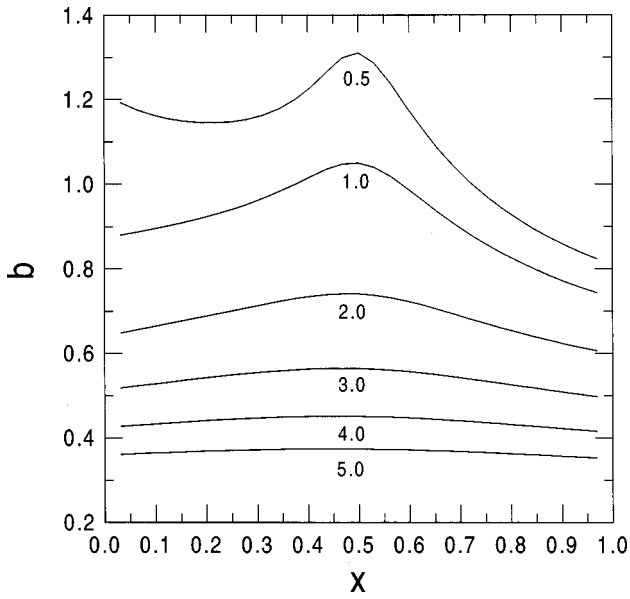

FIG. 12. The variational parameter b as a function of the doping.

the pattern expected for a collective charge mode, as described by the HCB and the DHCB models. For a doping $x \sim 1/2$, the kinetic energy reaches an absolute minimum which is independent of the values of the coupling constants. This optimal doping corresponds essentially to the maximum of the curve in Fig. 8, which gives the exponent of the exponential law governing the number of dimer-hole states.

The nature of the variational many-body state we have constructed is clarified by Figs. 11, 12, and 13 where we show the values of the variational parameters u, b, and c as functions of the doping x for different coupling constants. The parameter u starts from a positive value corresponding to the undoped ladder,[10] and it decreases upon doping until a critical value $x_c(J/J')$, where it vanishes. For higher dopings u becomes negative. For the undoped ladder the parameter u can be interpreted as the square of the RVB amplitude h_{RVB} for having a bond along the legs.[10] The analog amplitude for a bond along the rungs has been implicitly normalized to 1. For low doping, i.e., $x<x_c$, since $u(x)>0$, we can similarly define a doping-dependent amplitude for a leg bond as

$$u(x)=h^2_{\mathrm{RVB}}(x)>0 \quad (x<x_c). \tag{20}$$

In order to fulfill the Marshall theorem for the undoped ladder one requires the RVB amplitude $h_{\mathrm{RVB}}(0)$ to be positive,[8] which explains why $u(0)$ is also positive. Actually for the positivity of $u(0)$ one just needs $h_{\mathrm{RVB}}(0)$ to be a real number. At $x=0$, $h_{\mathrm{RVB}}(0)$ increases with J/J' due to the resonance between rung and leg singlets, according to the RVB scenario. Upon doping, however, the holes give rise to de-

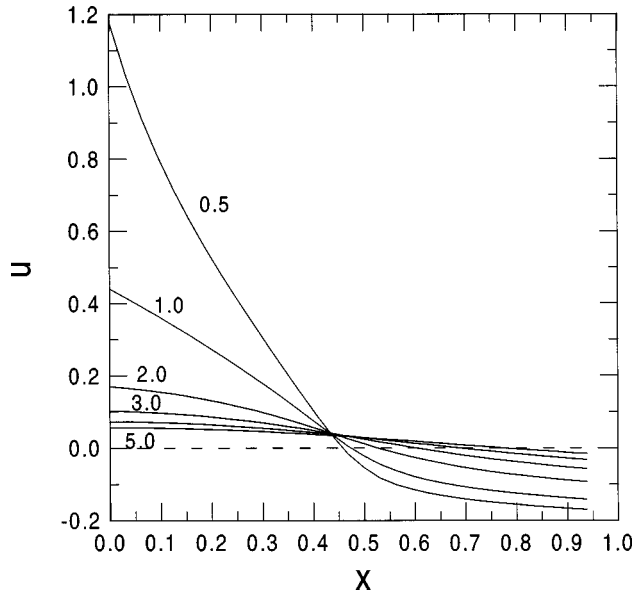

FIG. 11. The variational parameter u as a function of the doping.

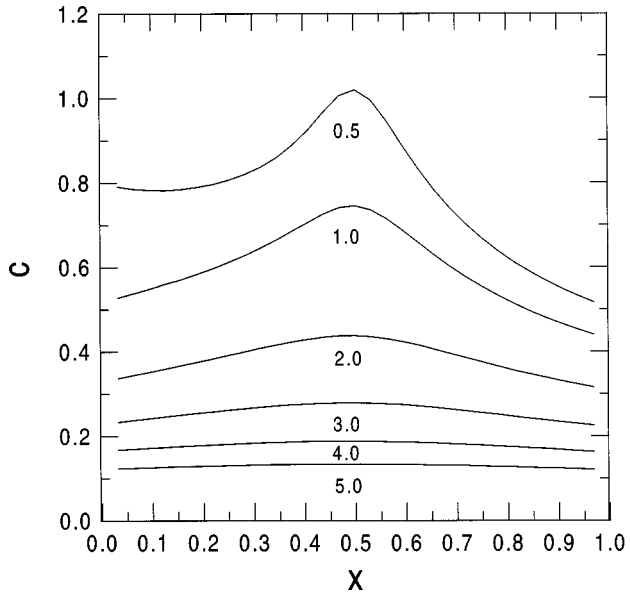

FIG. 13. The variational parameter c as a function of the doping.

structive interference which degrades progressively the aforementioned resonance mechanism. This explains why $u(x)$ and $h_{\mathrm{RVB}}(x)$ decrease with x. For $x<x_c$ the ground state is dominated by the resonating valence bonds and the RVB picture remains qualitatively correct.

For $x>x_c$ the interference due to the holes has driven u negative and it is no longer appropriate to interpret $u(x)$ as the square of h_{RVB}. Rather, the physical interpretation of the overdoped region comes from the solution of the Cooper problem in the t-J, two-leg ladder and its BCS extension. It can be shown analytically that two electrons in the latter system form a bound state only under certain conditions (details will be given elsewhere). For $J=0.5$, $t=t'=1$ one must have $J'>3.3048$ [note that the binding of two electrons in the t-J chain requires $J/2t>1$ (Ref. 14)]. The exact solution for four or more electrons is difficult to construct, but we expect it to be given essentially by a Gutzwiller-projected BCS-like wave function. A short-range version of the latter type of wave function can be generated from the recursion relation (8), with u a negative parameter, which can be written as

$$u(x)=-h_{\mathrm{BCS}}^2(x)<0 \quad (x>x_c), \tag{21}$$

where h_{BCS} is the BCS amplitude for finding two electrons at distance 1 along the legs. Of course this interpretation of u as minus the square of a BCS amplitude requires it to be negative. As we put more electrons into the ladder the value of h_{BCS} decreases, and for electron densities larger than $1-x_c$, we switch into the RVB regime.

The difference between the underdoped and overdoped regimes can be attributed to two different internal structures of the pairs. In the low-doping regime $x<x_c$, holes doped into the spin-liquid RVB state form pairs with an internal $d_{x^2-y^2}$-like structure relative to the undoped system. However, for $x>x_c$ one moves into the low density limit characterized by electrons doped into an internal s-wave-like symmetry. This issue will be discussed in detail in a separate publication.

Let us now comment on Figs. 12 and 13. Both are very similar and show that for $x\sim 1/2$, b and c reach their maximum. At $x=1/2$ there are as many electrons as holes, and in a certain sense the ground state of the ladder is a large-scale reproduction of the microscopic ground state of the 2×2 cluster given in Fig. 4. Indeed for $J=J'=0.5$, $t=t'=1$ the ratio b/a of the parameters appearing in Fig. 4 is given by 1.30, which is very close to the value of b at its maximum. For $x<0.7$ and $J'=0.5$ the parameter b is larger than 1 and it is always larger than c for all dopings and couplings. This is in agreement with the DMRG results of Ref. 9, which show the importance of the diagonal frustrating bonds above the horizontal or vertical ones for $J/t=J'/t=0.5$.

Finally Fig. 14 is a J/t-n diagram which shows the boundary of phase separation obtained by means of the DMRG method and the RRM in the case where $J=J'$, $t=t'=1$. Observe that this is not the strong-coupling case we have been discussing so far, and hence the validity of the RRM is more questionable.

The DMRG phase separation boundary was calculated using many different simulations on large ladders with open boundary conditions. Phase separation on a large open ladder

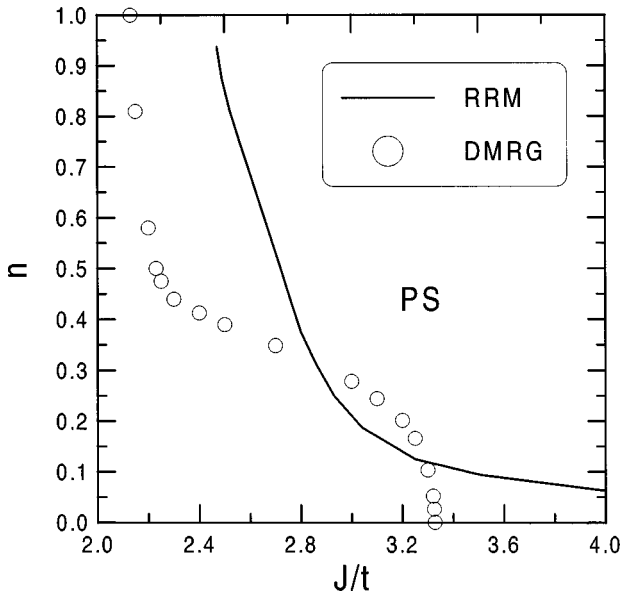

FIG. 14. Boundary of the phase separation region in the case where $J=J'$, $t=t'$, computed with the DMRG method and the RRM.

is easily observed—the holes form either a single hole-rich region in the center or two hole-rich regions on the ends, with the rest of the system hole free. The density of holes in the hole-rich region gives a point on the phase separation boundary. For most values of J/t relatively short ladders (32×2) could be used, since the hole density decayed quickly with distance to a single value near the ''surface'' of the hole-rich region. Near $J/t\sim 2.15$, the surface was much less sharp and systems as large as 256×2 were needed. In this case many DMRG sweeps were also needed to equilibrate the hole density.

Within the RRM, the phase-separated state is constructed as the composition of two phases: one is a hole-rich phase and the other phase is a hole-free phase with only spins.

The energy of this state can be written as

$$e_{N,P}^{\mathrm{sep}}=e_{N-P-l,0}+e_{P+l,P}, \quad \left(e_{N,P}=\frac{E_{N,P}}{Z_{N,P}}\right), \tag{22}$$

where l counts the number of fermion pairs in the hole-rich phase. We have used the RRM to calculate the energy in both phases looking for a minimum of e_{NP}^{sep} in l. Once the minimum is achieved, the phase-separated energy is compared with the uniform phase energy to determine which of the two phases is more stable.[15]

We obtain an overall agreement between the results obtained with the DMRG method and the RRM (see Refs. 6, 16, and 17 for comparisons with other numerical results). In the two-leg t-J model, phase separation is controlled by J, rather than J', and so the strongest coupling we have considered above, $J'/t=5$, $J/t=0.5$, $t'/t=1$, does not phase separate.

CONCLUSIONS

In this paper we have proposed an extension of the effective hard-core boson model of the two-leg ladder of Ref. 6, in order to include the local structure of the hole pairs. The

extended effective model, called the DHCB model, contains dimer bonds, hard-core bosons, and various combinations between bonds and holes, whose relevance have been studied previously with the DMRG method.[9] Generalizing the methods of Ref. 10 to the case with holes, we study a variational ansatz for the ground state of the DHCB model, which depends only on three variational parameters. The resulting dimer-hole state is generated by a second-order recursion formula, which also leads to recursion formulas for the overlaps necessary to compute the energy of the ansatz. We give the results of the energy minimization for the 2×32 ladder and compare them with those obtained with the DMRG method in the strong-coupling region. The recursion relations we have derived for the ground state energy can be solved analytically in the thermodynamic limit and the minimization can then be done numerically. Finally we give a physical interpretation of the behavior of the variational parameters with doping.

ACKNOWLEDGMENTS

G.S. would like to thank the organizers of the ITP program ''Quantum Field Theory in Low Dimensions: From Condensed Matter to Particle Physics'' for the warm hospitality. M.A.M.D. thanks the organizers of the Benasque Center of Physics 1997 for their support and hospitality. G.S. acknowledges support from the NSF under Grant No. PHY94-07194 and the Dirección General de Enseñanza Superior, M.A.M.D. acknowledges support from the CICYT under Contract No. AEN93-0776, J.D. acknowledges support from the DIGICYT under Contract No. PB95/0123, S.R.W. acknowledges support from the NSF under Grant No. DMR-9509945, and D.J.S. acknowledges support from the NSF under Grant Nos. PHY-9407194 and DMR-9527304.

*On leave from Instituto de Matemáticas y Física Fundamental, C.S.I.C., 28006 Madrid, Spain. Electronic address: sierra@sisifo.imaff.csic.es
†Electronic address: mardel@eucmax.sim.ucm.es
‡Electronic address: emduke@iem.csic.es
§Electronic address: srwhite@uci.edu
‖Electronic address: djs@spock.physics.ucsb.edu

[1] E. Dagotto, J. Riera, and D. J. Scalapino, Phys. Rev. B **45**, 5744 (1992).
[2] T. Barnes, E. Dagotto, J. Riera, and E. S. Swanson, Phys. Rev. B **47**, 3196 (1993).
[3] S. Gopalan, T. M. Rice, and M. Sigrist, Phys. Rev. B **49**, 8901 (1994).
[4] S. R. White, R. M. Noack, and D. J. Scalapino, Phys. Rev. Lett. **73**, 886 (1994).
[5] H. Tsunetsugu, M. Troyer, and T. M. Rice, Phys. Rev. B **49**, 16 078 (1994).
[6] M. Troyer, H. Tsunetsugu, and T. M. Rice, Phys. Rev. B **53**, 251 (1996).
[7] S. A. Kivelson, D. S. Rokhsar, and J. P. Sethna, Phys. Rev. B **35**, 8865 (1987).
[8] S. Liang, B. Doucot, and P. W. Anderson, Phys. Rev. Lett. **61**, 365 (1988).
[9] S. R. White and D. J. Scalapino, Phys. Rev. B **55**, 6504 (1997).
[10] G. Sierra and M. A. Martín-Delgado, cond-mat/9704212, Phys. Rev. B. (to be published).
[11] Y. Fan and M. Ma, Phys. Rev. B **37**, 1820 (1988).
[12] R. Baxter, *Exactly Solved Models in Statistical Mechanics* (Academic Press, London, 1982).
[13] S. R. White, Phys. Rev. Lett. **69**, 2863 (1992); Phys. Rev. B **48**, 10 345 (1993).
[14] M. Ogata, M. U. Luchini, S. Sorella, and F. F. Assaad, Phys. Rev. Lett. **66**, 2388 (1991).
[15] V. J. Emery, S. A. Kivelson, and H. Q. Lin, Phys. Rev. Lett. **64**, 475 (1990).
[16] C. A. Hayward and D. Poilblanc, Phys. Rev. B **53**, 11 721 (1996).
[17] K. Sano, J. Phys. Soc. Jpn. **65**, 1146 (1996).